Mem. S.A.It. Vol. 81, 646

Memorie della

Photometric analysis of Ellerman bombs

A. Berlicki[1,2], P. Heinzel[1], and E. H. Avrett[3]

[1] Astronomical Institute, Academy of Sciences, 25165 Ondřejov, Czech Republic
e-mail: berlicki@astro.uni.wroc.pl
[2] Astronomical Institute, University of Wrocław, ul. Kopernika 11, 51-622 Wrocław, Poland
[3] Harvard-Smithsonian Center for Astrophysics, 60 Garden Street, Cambridge, MA 02138, USA

Abstract. Observations of Ellerman bombs (EBs) show them as short-lived, compact, and spatially localized emissions that are well observable in the wings of the Hα hydrogen line. The Hα line profiles of EBs are characterized by deep absorption at the line center and enhanced emission in the wings with maximum around ±1 Å from the line center, fading beyond ±5 Å. EBs may also be observed in the chromospheric Ca II lines and in the UV as bright points often located within active regions. Previous work suggests that EBs may be considered as micro-flares and may contribute significantly to the heating of the lower chromosphere in newly emerging magnetic flux regions. However, it is still not clear at what height in the solar atmosphere the emission of EBs originates. In our analysis we used observations of EBs obtained in the Hα line with the Dutch Open Telescope (DOT) and in the UV range with the TRACE 1600 Å channel. These one-hour long simultaneous sequences obtained with high temporal and spatial resolution were used to analyze the relation between the emission in the Hα line and at 1600 Å. The observations show fast variations of EB emission in both channels. Comparison between the observed emission in Hα and at 1600 Å and theoretical calculations allowed us to draw conclusions about the vertical structure of EBs.

Key words. Line: formation – Methods: numerical – Techniques: spectroscopic – Sun: chromosphere

1. Introduction

Ellerman bombs (EBs) were first described by Ellerman (1917). EBs are small-scale structures observed in the wings of the Hα line and in the UV continuum which originates from the temperature minimum region. Ellerman described them as bright, compact structures of a few minutes lifetime, which can by seen on spectrograms in the range 4–15 Å from the center of the Hα line (Fig. 1).

EBs are often observed in regions of magnetic flux emergence. They occur not only in new active regions but also in old ones in places where the magnetic field starts to rebuild. They can be seen near sunspots, arch filament systems as well as in large superpenumbrae. Zachariadis et al. (1987) show that about half of all EBs appear in pairs. Moreover these pairs have a tendency to orient themselves par-

Send offprint requests to: A. Berlicki

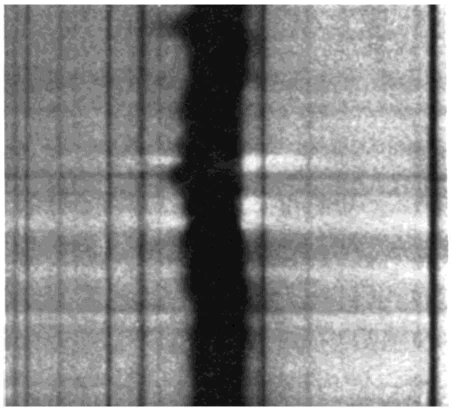

Fig. 1. Appearance of the Hα line showing the emission of Ellerman bomb – long wings on both sides of the line (from Ellerman 1917). The spectral range covered in the image is 13 Å.

allel to large scale magnetic structures in the active region. Georgoulis et al. (2002) found that EBs have a tendency to concentrate above magnetic neutral lines outlining the boundaries of supergranular cells or in moving dipolar features (MDF, see Bernasconi et al. 2002).

The average lifetime of EBs typically is a dozen of minutes (Severny 1956; McMath et al. 1960; Roy & Leparskas 1973; Kurokawa et al. 1982), but there are also observations of EBs lasting for more than half an hour (Roy & Leparskas 1973; Kurokawa et al. 1982; Qiu et al. 2000; Pariat et al. 2007). The light curves of those EBs which were observed for more than 20 minutes seem to consist of several maxima or show one flat maximum with some oscillation in brightness (Roy & Leparskas 1973; Kurokawa et al. 1982). Analysis of the evolution of EBs observed in UV 1600 Å by Qiu et al. (2000) showed that EBs show a variation in brightness on short time scales of 1–5 minutes . In their analysis Pariat et al. (2007) showed that 88% of individual impulses have a lifetime between 100 and 430 seconds, with a preferred value of 210 seconds.

Besides the Hα line, EBs are also observed in other chromospheric lines like the Ca II H line. Examples of line profiles of EBs in both Hα and Ca II 8542 Å lines were shown in Fang et al. (2006) and Pariat et al. (2007).

The line profiles and continua observed in EBs are used to construct models of the atmosphere within these structures. The results of such modeling imply that the whole region of EBs is hotter in comparison to the quiet solar atmosphere, and the heating is significant only in the lower chromosphere where the Hα line wings and the UV continuum are formed. Fang et al. (2006) obtained a semi-empirical model of EBs and concluded that EBs require a temperature increase of about 600–1 300 K in the lower atmosphere close to the temperature minimum region. They also calculated that the energy of EBs is about 10^{26} to 5×10^{27} erg, and they suggest that EBs could be similar to nanoflare events. The MHD studies of Georgoulis et al. (2002) and Pariat et al. (2004, 2009) led to a similar conclusion.

In this study we aim to confirm that EBs are formed in the lower solar atmosphere. Previous observations show that EB emission is enhanced in the line wings of chromospheric lines which was taken as an indication that EBs should form close to the temperature minimum region. Theoretical modeling indicates that not only the wings of chromospheric lines are formed in these layers but also the UV continuum. Therefore, we used Hα observations and the UV continuum at 1600 Å to study the emission of EBs. We compare the time evolution of these emissions and use them to estimate the temperature structure of EBs. Using NLTE calculations we simulate the observed emission to find possible models of EBs.

2. Observations of Ellerman bombs

After inspection of Dutch Open Telescope (DOT; Rutten et al. 2004) and TRACE databases we found a series of observations obtained in the Hα line wings and in the UV at 1600 Å that were adequate for our analysis. These observations concerned the active region NOAA 10892 and were obtained on 2006 June 7 (Fig. 2).

The series of DOT and TRACE observations were simultaneously obtained between 08:20 and 09:30 UT with a cadence of about

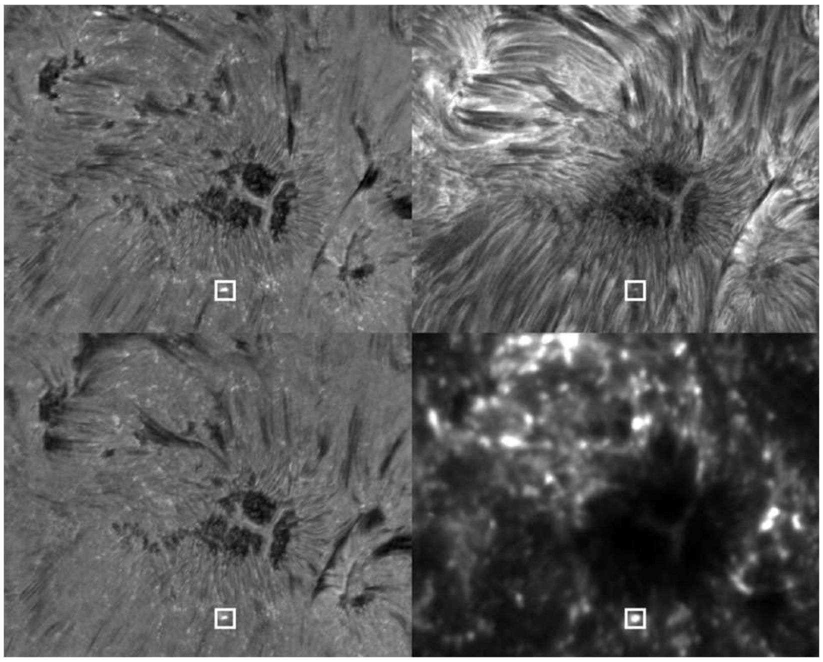

Fig. 2. Active region NOAA 10892 observed at 08:25 UT. One of the analyzed EBs is marked with the square. Upper left: DOT Hα −0.7 Å, Upper right: DOT Hα line center, Lower left: DOT Hα +0.7 Å, Lower right: TRACE 1600 Å.

30 seconds. The DOT data consists of 134 images at three different wavelengths in the Hα line (−0.7 Å, line center, +0.7 Å). We used these 402 images , which were all co-aligned and saved in one data cube. The TRACE sequence consists of 146 images but those acquired between 09:00-09:15 UT were not used because of calibration problems. Next, we co-aligned the DOT Hα images with the TRACE 1600 Å data. The accuracy of the co-alignment is around 1″. Finally, we obtained almost simultaneous and co-aligned DOT and TRACE sequences. The maximum time difference between corresponding DOT and TRACE images is less than 20 seconds.

3. Analysis of the intensities of Ellerman bombs

In order to analyze the time evolution of intensities of EBs, we first searched for small, compact emissions in the DOT images obtained in the Hα line wings. During the period 08:20–09:30 UT we were able to find more than ten such events. These small structures were clearly visible in the DOT images taken in the Hα line wings but they were less visible or almost absent in the Hα line center, which agrees with the typical appearance of EBs. In addition, all of them were also visible in the corresponding TRACE 1600 Å images. In Fig. 2 we show an example of such an EB. The EB marked with the square is very well visible in DOT images at H$\alpha \pm 0.7$ Å and is also bright in TRACE 1600 Å. Brightening associated with this EB in the Hα line center is negligible. In case of other EBs similar behavior was observed.

For all the EBs found in the analyzed period of time we constructed plots showing the time evolution of their emission in the Hα line and in UV continuum at 1600 Å. For better comparison of the data from different instru-

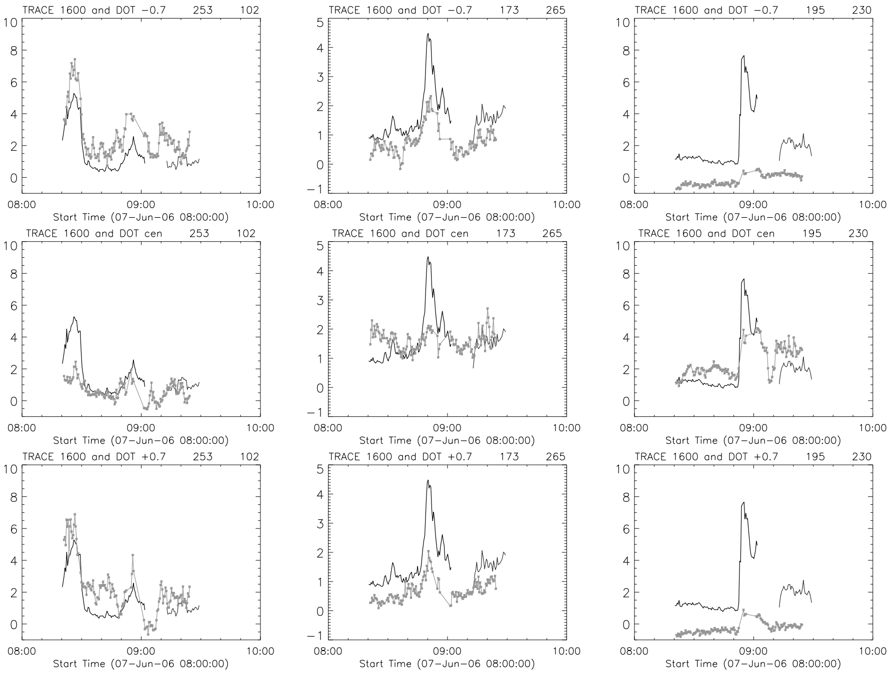

Fig. 3. Time evolution of the intensity contrast C plotted for two specific Ellerman bombs (two first columns) and for the area with flare-like emission (third column). Thin black lines in all panels: TRACE 1600 Å emission contrast. Grey lines with dots mark the contrast of EBs or flare-like emissions in the Hα − 0.7 Å (upper panel), in the Hα line center (middle raw) and in the Hα + 0.7 Å (lower panel). For better visibility the Hα contrast is multiplied by the factor 10 (first column), 5 (second column) and 3 (third column).

ments we used the contrast intensities defined as:

$$C = \frac{I_{\rm EB} - I_{\rm QS}}{I_{\rm QS}}. \quad (1)$$

In order to reduce noise and a possible influence of bad co-alignment we integrate the signal over small boxes containing the analyzed EB.

In the first and second column of Fig. 3 we show examples of time evolution of the contrast intensities for two EBs. In each column we plot UV 1600 Å contrast of EBs and Hα contrast in the line center and in both wings. Note that for better visibility, the Hα contrast is multiplied by factor 10 (first column), 5 (second column) and 3 (third column). The contrast in 1600 Å is not multiplied by any factor. In the left column we show EB which had a maximum at 08:25 UT, in the second column the EB with the maximum at 08:50 UT. In both cases it is easy to notice good correlation between the increased contrast observed in the Hα line wings at ±0.7 Å and in UV at 1600 Å. The increase of the contrast in the Hα line center is much lower. In the left column another contrast peak is visible around 08:55 UT. It is smaller than the previous one but again the increase of the Hα contrast is higher in the line wings than in the line center. Probably, we observed new EB in the same position as that observed at 08:25 UT.

For all these EBs we obtained the mean contrast at ±0.7 Å: $C_{\rm H1} = 0.7$ for EB observed at 08:25 UT, $C_{\rm H2} = 0.5$ for EB observed at 08:50 UT and $C_{\rm H3} = 0.4$ for EB observed at 08:55 UT. The corresponding contrast of the UV 1600 Å emission observed with TRACE is the following: $C_{\rm T1} = 5.5$, $C_{\rm T2} = 4.5$ and $C_{\rm T3} = 3.0$. All these values will be compared

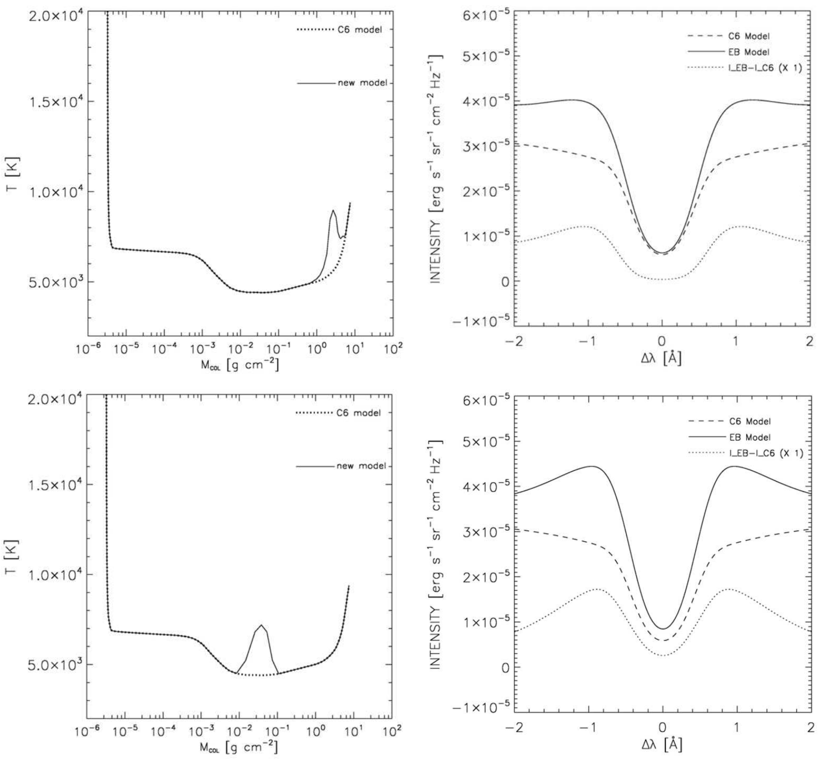

Fig. 4. Two proposed models of the temperature structure in EBs (left) and the corresponding theoretical Hα line profiles (right). Upper panel: Model 1. Lower panel: Model 2. For comparison we also plotted the temperature of the reference quiet-Sun model C6 (Avrett 2007) (left panel, dotted line) and corresponding line profile (right panel, dashed line).

with the theoretical calculations in the next section.

During the analyzed time period, we also identified some bright compact areas in the DOT Hα images which exhibited high contrast in the line center and low contrast in the line wings (Fig. 3, third column). This behavior is opposite to that in EBs and thus suggests a different mechanism. .

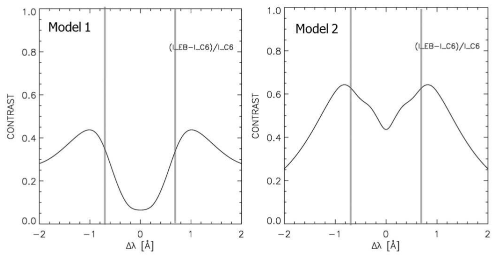

Fig. 5. Hα line contrast profiles calculated for Model 1 (left) and Model 2 (right) of Ellerman bombs. The grey vertical lines mark the positions of bandpasses in the wings of the line as observed by the Hα tunable filter at Dutch Open Telescope.

4. Theoretical simulations

We try to simulate the observed emission of EBs using NLTE numerical codes (Heinzel 1995; Avrett & Loeser 2008) which allow us to compute the emergent Hα line profiles and the UV continuum for any input model of the solar atmosphere. Based on the previous work of, e.g., Fang et al. (2006), we construct two

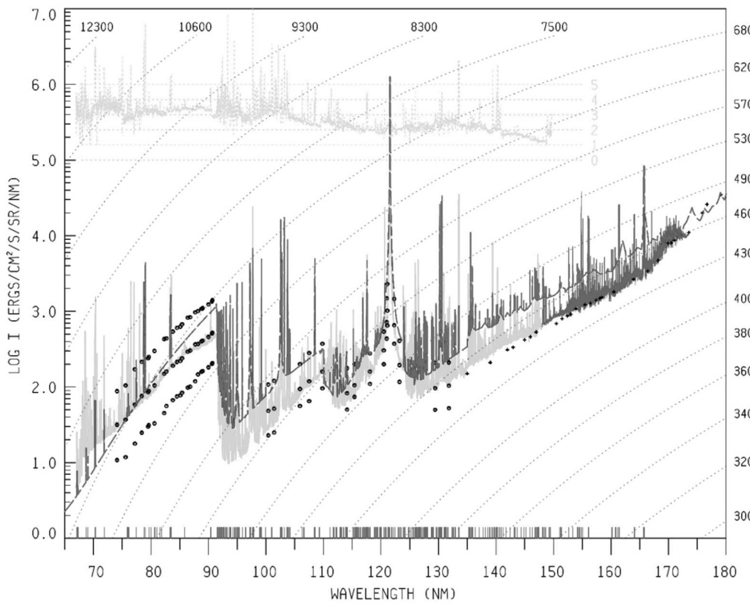

Fig. 6. The SUMER disk-center spectrum (light grey) of the average quiet Sun between 67 and 147 nm is plotted with the calculated spectrum (dark-grey long dashes). The calculated spectrum comes from a model with temperatures 200 K higher than those of the C6 model throughout the chromosphere and temperature-minimum region. For more details see Avrett (2007).

models which are supposed to correspond to the atmospheric structure in EBs. The column mass–temperature structure of these models is presented in Fig. 4 (left column). EBs are characterized by a temperature increase close to the photosphere (Model 1) or in the temperature minimum region (Model 2). The maximum increase of the temperature is about 3 000 K. In the right column of Fig. 4 we show the synthesized Hα line profiles corresponding to these two models. Both line profiles exhibit strong excess of emission in the line wings around ±1.0 Å. These theoretical line profiles still have enhanced emission even far beyond 1.0 Å and they are similar to those observed in EBs. It is worth noting that the emission in the line core is almost unaffected.

To compare the calculations with the DOT observations, we calculate the contrast at ±0.7 Å (DOT bandpasses) from these theoretical Hα line profiles we calculated the contrast at ±0.7 Å (DOT bandpasses). We obtain (see Fig. 5): $C = 0.35$ for Model 1 and $C = 0.6$ for Model 2. Both values are similar to those observed in EBs described in the previous section.

Using Models 1 and 2 of EBs we also calculate the theoretical contrast for the UV emission around 1600 Å. We find $C = 0.2$ for Model 1 and $C = 15$ for Model 2. In this case, only Model 2 shows an intensity contrast which is high enough to be comparable with the TRACE 1600 Å observations edd aken with TRACE. The UV contrast in Model 1 is almost not affected.

5. Discussion and conclusions

In this paper we use observations of EBs obtained in the Hα line and in the UV around 1600 Å to propose a model of EBs which could reasonably reproduce the observed features. These observations showed that there is a good temporal and spatial correlation between the EB emission observed in the wings of the Hα line and in the UV around 1600 Å. This correlation suggests that both types of emission come from the same places in the solar atmosphere. High contrast of EB emission observed in the Hα line wings and weak contrast in the line center gives us certain evidence that EBs are located in the lower atmosphere, below the areas where the quiet-Sun Hα line core is formed. Probably, it is close to the temperature minimum region. Observations of the UV emission around 1600 Å seem to support this idea because this continuum emission is also formed at the base of the chromosphere.

In this context it is easy to explain the case presented in the third column of Fig. 3 where we find a strong intensity contrast only in the Hα line core and in the UV at 1600 Å. Probably, this is a flare-like emission which is produced at the top of the chromosphere and therefore only the Hα line-core emission is enhanced. The UV emission at 1600 Å is also stronger but this effect is not caused by the enhanced UV continuum emission but by the hotter transition region lines which are much stronger in flare-like phenomena. There are many such lines which contribute to the total emission in the UV (Fig. 6). In EB the increase of the intensity in the UV range around 1600 is due to the continuum emission excess, but in flare-like event this increase is due to the line emission excess. This duality follows from the different heights where the emission of EB and flare-like features is formed.

The observed Hα and UV contrast allows us to find a model of EBs which is characterized by a local temperature enhancement in the lower chromosphere. We propose two models with different locations of such temperature increase. Although both, Model 1 and Model 2, well reproduce the contrast observed in the Hα line wings, only Model 2 gives a similar contrast to that observed in the the UV 1600 Å emission. Therefore, we suggest that the temperature increase which is responsible for the appearance of EBs should be located in the temperature minimum region. Simultaneously, the remaining part of the solar atmosphere should not be strongly affected.

For future work, it is necessary to use spectroscopic observations of EBs obtained in lines and continua. It is also important to construct models without the assumption of hydrostatic equilibrium, and with different geometries. The UV emission should be treated in more detail including analysis of the ambiguity between continuum and line emissions within this spectral range.

Acknowledgements. The work of A.B. was supported by the Polish Ministry of Science and Higher Education, grant N203 016 32/2287 and by the grant of Czech Academy of Sciences, No. M100030942. We would like to thank the Dutch Open Telescope team for the data and especially to Rob Rutten for valuable discussions.

References

Avrett, E. H. 2007, in The Physics of Chromospheric Plasmas, ed. P. Heinzel, I. Dorotovič, & R. J. Rutten, PASPC, 368, 81

Avrett, E. H. & Loeser, R. 2008, ApJS, 175, 229

Bernasconi, P. N., Rust, D. M., Georgoulis, M. K., & Labonte, B. J. 2002, Sol. Phys., 209, 119

Ellerman, F. 1917, ApJ, 46, 298

Fang, C., Tang, Y. H., Xu, Z., Ding, M. D., & Chen, P. F. 2006, ApJ, 643, 1325

Georgoulis, M. K., Rust, D. M., Bernasconi, P. N., & Schmieder, B. 2002, ApJ, 575, 506

Heinzel, P. 1995, A&A, 299, 563

Kurokawa, H., Kawaguchi, I., Funakoshi, Y., & Nakai, Y. 1982, Sol. Phys., 79, 77

McMath, R. R., Mohler, O. C., & Dodson, H. W. 1960, Proc. of the National Academy of Science, 46, 165

Pariat, E., Aulanier, G., Schmieder, B., et al. 2004, ApJ, 614, 1099

Pariat, E., Masson, S., & Aulanier, G. 2009, ApJ, 701, 1911

Pariat, E., Schmieder, B., Berlicki, A., et al. 2007, A&A, 473, 279

Qiu, J., Ding, M. D., Wang, H., Denker, C., & Goode, P. R. 2000, ApJ, 544, 157

Roy, J.-R. & Leparskas, H. 1973, Sol. Phys., 30, 449

Rutten, R. J., Hammerschlag, R. H., Bettonvil, F. C. M., Sütterlin, P., & de Wijn, A. G. 2004, A&A, 413, 1183

Severny, A. B. 1956, The Observatory, 76, 241

Zachariadis, T. G., Alissandrakis, C. E., & Banos, G. 1987, Sol. Phys., 108, 227